M2AN - MODÉLISATION MATHÉMATIQUE ET ANALYSE NUMÉRIQUE

D. CHOI
F. J. PALMA
E. SANCHEZ-PALENCIA
M. A. VILARIÑO

Membrane locking in the finite element computation of very thin elastic shells

M2AN - Modélisation mathématique et analyse numérique, tome 32, n° 2 (1998), p. 131-152

<http://www.numdam.org/item?id=M2AN_1998__32_2_131_0>

MATHEMATICAL MODELLING AND NUMERICAL ANALYSIS
MODELISATION MATHÉMATIQUE ET ANALYSE NUMÉRIQUE

(Vol 32, n° 2, 1998, p 131 à 152)

MEMBRANE LOCKING IN THE FINITE ELEMENT COMPUTATION OF VERY THIN ELASTIC SHELLS (*)

by D. CHOI (1), F. J. PALMA (2), E. SANCHEZ-PALENCIA (1), M. A. VILARIÑO (2)

Abstract — *The membrane locking phenomenon arises in cases when the middle surface of the shell admits "pure bendings" satisfying the kinematic boundary conditions It then appears that the discrete approximations by finite elements is unsuited to describe such pure bendings, which are the limit configuration of solutions as the thickness tends to zero This phenomenon is described in terms of lack of robustness (i e lack of uniformity of the finite element convergence $h \searrow 0$ with respect to the thickness of the shell 2ε) We prove that any finite element scheme consisting of in piecewise polynomial functions necessarily exhibits locking for certain shells (and probably for almost any shell admiting pure bendings) Numerical experiments are done for a hyperbolic paraboloid The superiority of schemes involving high order polynomials (Ganev-Argyris in particular) is shown It is also seen that reduced integration have very little influence on membrane locking*

Résumé. — *Le phénomène de verrouillage membranaire intervient lorsque la surface moyenne de la coque admet des « flexions pures » satisfaisant aux conditions aux limites cinématiques Dans ce cas les approximations discrètes par éléments finis sont inappropriées pour décrire ces flexions pures, qui sont les configurations limites des solutions lorsque l'épaisseur tend vers zéro Le phénomène est décrit en terme de manque de robustesse (ou manque d'uniformité de la convergence des éléments finis $h \searrow 0$ par rapport à l'épaisseur de la coque 2ε) Nous démontrons que tout schéma éléments finis qui consiste dans des fonctions polynomiales par morceaux, présente nécessairement le phénomène de verrouillage pour certaines surfaces (et probablement pour presque toutes les surfaces admettant des flexions pures). On a fait des exemples numériques pour le paraboloide hyperbolique, montrant la supériorité des schémas qui font intervenir des polynômes de degré élevé (Ganev-Argyris en particulier) On voit aussi que l'intégration réduite a une très petite influence sur le verrouillage membranaire*

1. INTRODUCTION

It is known that the phenomenon of membrane locking in numerical computation of thin shells consists in an inadequacy of the finite elements to describe the very peculiar deformations of a shell [15], [10], [6], [9]. Actually, the natural trend of a thin shell is to perform pure bendings, i.e. inextensional displacements of the middle surface (which do not modify the intrinsic metrics of the middle surface), but the explicit description of the phenomenon and the above mentioned inadequacy of the finite element approximation usually lack in the litterature.

The asymptotic study of the behavior of elastic shells as the thickness 2ε tends to zero [15], [16], [17] shows two very different asymptotic behaviors in the cases when the medium surface with the kinematic boundary conditions admits or no inextensional displacements. In the former case, the shell is called to be "non-inhibited" (for "with non-inhibited pure bendings") and in the later it is said to be "inhibited" (for "with inhibited pure bendings"). It should be noticed that the concept of "inhibited" coincides with that of "geometrically rigid", but we adopt the term "inhibited", as "rigidity" is a different concept in mechanics of continua.

It then appears that the membrane locking only occurs in non-inhibited shells. This elementary assertion is nevertheless useful to introduce a little order in the comments on locking which are usually encountered in the literature. For instance in [3], p. 238-239 are considered three examples of shells which are taken as benchmarks

(*) Manuscript received September 16, 1996

(1) Laboratoire de Modélisation en Mécanique, Université Pierre et Marie Curie, 4 place Jussieu, 75252 Paris Cedex 05 (France)

(2) Departamento de Analisis Matematico, Facultad de Ciencias, Campus de Teatinos, 29071 Malaga (Spain).

This work is part of the "Action intégrée franco-espagnole PICASSO 95-96" This work is also part of the of the Human Capital and Mobility Program "Shells Mathematical Modelling and Analysis, Scientific Computing" of the Commission of the European communities (contract ERBCHRXCT 940536).

for testing the adequacy of finite element methods but only the third one (semi-sphere with free boundary) is non-inhibited; the others are not concerned with membrane locking. Moreover, no tests are given for very thin shells, when membrane locking is an asymptotic phenomenon for small thickness. It should also be mentioned that arches, which are the two-dimensional counterparts of shells are always non-inhibited, and the corresponding locking is simpler and better known [6].

It is a remarkable fact that a shell is, by definition, thin, but nevertheless, the equations of classical theory of shells (see, for instance [13], [4]) contain two terms corresponding to the deformation energies of membrane strain and flexion. The corresponding coefficients are in a ratio ε^{-2} as the membrane rigidity is higher than the flexion one. Consequently we may study the asymptotic behavior of a thin shell as $\varepsilon \searrow 0$ ([15], [16], [17] already mentioned). The classical convergence of the finite element approximation as the mesh diameter h tends to zero [4] holds true for fixed ε, but the constants appearing in the convergence estimates depend on ε. Babuska and Suri define the locking [1] as the non-uniformity of the convergence with respect to ε. They also call "robust" an approximation method when the convergence $h \searrow 0$ is uniform with respect to a parameter ε. Locking is in fact lack of robustness. This definition, which we adopt in this paper, seems to be quite fitted as an approximation method in theory of shells, which are naturally thin, should convergence quite well for any value of the small thickness.

Otherwise one must change the mesh diameter when changing the thickness. We shall see that this is the general situation, and the values of h which are necessary to get a good approximation with small ε are impracticable. The paper [10] by Kamoulakos is quite interesting in this context. After giving a review of the work accomplised mainly by L.S.D. Morley, he considers a specific type of quadrangle finite elements and shows that the appropriate h should be of order ε or even ε^2 in certain directions! He also exhibits finite elements computations of shell stresses with errors going from 2 % to 46 000 %!

We also notice that the locking phenomenon seems also be present in a variety of approximation methods. See for instance [9], [6], [11] for the approximation of arches by straight beam elements and [1] for approximation of shells by plane facets.

In this paper we adopt a view point very close to that of Chenais and Paumier [6] but we consider the case of shells instead of that of arches. Our main result (section 4) is that any finite element internal approximation made of functions which are piecewise polynomials leads to locking for certain surfaces such as the hyperbolic paraboloid and the straight helicoid. The proof relies on incompatibilities involving explicit expressions of the equations for these surfaces. We also show in a less rigorous way (begining of section 4) that generally speaking, thereis incompatibility between the pure bendings and the finite dimensional space V_h of the finite element approximation from which the general character of the locking phenomenon follows.

The previous considerations are then extended (section 5) to a widely used kind of non-conforming finite elements, the so-called DKT (= Discrete Kirchhoff Triangle) approximation.

Section 6 is devoted to numerical experiments. We chose a non-inhibited shell (a hyperbolic paraboloid with appropriate boundary conditions) which is not the case in a part of the usual benchmarks. Computations were done for two finite element schemes: Ganev-Argyris (conformal, using high order polynomials) and Sander (non-conformal, with lower oder polynomials). For each one, several different integration schemes were considered. Numerical results show the superiority of higher order polynomials. Indeed, fairly good computations were obtained with an Apollo station for $\varepsilon > 10^{-3}$ (Ganev-Argyris) and $\varepsilon > 10^{-2}$ (Sander), where $2\varepsilon =$ thickness. Otherwise, very little influence of the integration schemes was observed, contrary to the wide-spread opinion that reduced integration diminishes locking effects.

2. SETTING OF THE PROBLEM. ROBUSTNESS AND LOCKING

Let us first state the shell problem in the framework of Koiter theory (see for instance [4]). Let E^3 be the Euclidean space referred to an orthonormed frame $(\mathbf{e}_1, \mathbf{e}_2, \mathbf{e}_3)$ and let Ω be a bounded open set of $\mathbb{R}^2$ with boundary Γ. The middle surface of the shell (denoted by S) is the image in E^3 of $\overline{\Omega}$ by the map

$$\boldsymbol{\varphi} : (y^1, y^2) \in \overline{\Omega} \to \boldsymbol{\varphi}(\mathbf{y}) \in E^3 \tag{2.1}$$

At each point of S we consider the two tangent vectors

$$\mathbf{a}_\alpha = \boldsymbol{\varphi}_{,\alpha} \equiv \partial\boldsymbol{\varphi}/\partial y^\alpha \equiv \partial_\alpha \boldsymbol{\varphi} \quad (\alpha = 1, 2) \tag{2.2}$$

(greek indices run from 1 to 2, and latin ones from 1 to 3. Note also the different notations used for partial differentiation). The unit normal vector to S is

$$\mathbf{a}_3 = \mathbf{a}_1 \times \mathbf{a}_2 / |\mathbf{a}_1 \times \mathbf{a}_2| \tag{2.3}$$

The map $\boldsymbol{\varphi}$, and then S are supposed to be smooth; we then consider, in a neighbourhood of S the "normal curvilinear coordinates" y^1, y^2, y^3 where y^3 is the distance to S along the normal. For the sake of simplicity we only consider the case of constant thickness $2\,\varepsilon$. The shell is then the set

$$C = \{M \in E^3, \quad M = \boldsymbol{\varphi}(y^1, y^2) + y^3\,\mathbf{a}_3, \quad (y^1, y^2) \in \overline{\Omega}, \quad |y^3| < \varepsilon\} \tag{2.4}$$

Let $\mathbf{u}(y^1, y^2)$ be the displacement vector of S when the shell is submited to forces $\varepsilon^3\,\mathbf{f}$ by unit surface. We only consider linearized theory for small $\mathbf{u}$. The Koiter theory is then described in terms of the linear term of the *membrane strain tensor*

$$\gamma_{\alpha\beta}(\mathbf{u}) = \frac{1}{2}(\bar{a}_{\alpha\beta} - a_{\alpha\beta}) \tag{2.5}$$

and of the linear terms of the *change of curvature tensor*

$$\rho_{\alpha\beta}(\mathbf{u}) = \bar{b}_{\alpha\beta} - b_{\alpha\beta}\,. \tag{2.6}$$

In the previous expressions, $a_{\alpha\beta}$(resp. $\bar{a}_{\alpha\beta}$) and $b_{\alpha\beta}$(resp. $\bar{b}_{\alpha\beta}$) denote the coefficients of the first and second fundamental forms of S before (resp. after) deformation, i.e.

$$a_{\alpha\beta} = \mathbf{a}_\alpha \cdot \mathbf{a}_\beta = \boldsymbol{\varphi}_{,\alpha} \cdot \boldsymbol{\varphi}_{,\beta} \tag{2.7}$$

$$b_{\alpha\beta} = -\,\mathbf{a}_\alpha \cdot \mathbf{a}_{3,\beta} = \mathbf{a}_3 \cdot \mathbf{a}_{\alpha,\beta} = \mathbf{a}_3 \cdot \mathbf{a}_{\beta,\alpha} \tag{2.8}$$

where, α denotes *differentiation* with respect to y^α. Correspondingly, the symbol $|\alpha$ will be used for *covariant differentiation.*

The contravariant basis $\mathbf{a}^\alpha$ is defined by

$$\mathbf{a}_\alpha \cdot \mathbf{a}^\beta = \delta_\alpha^\beta \tag{2.9}$$

where δ denotes the Kronecker symbol. The contravariant components of the metric tensor are

$$a^{\alpha\beta} = \mathbf{a}^\alpha \cdot \mathbf{a}^\beta\,. \tag{2.10}$$

They are used, as well as $a_{\alpha\beta}$ to pass from covariant to contravariant components of vectors and tensors in the usual way. The tensors γ and ρ are then:

$$\gamma_{\alpha\beta}(\mathbf{u}) = \frac{1}{2}(u_{\alpha|\beta} + u_{\beta|\alpha}) - b_{\alpha\beta}\,u_3 \tag{2.11}$$

$$\rho_{\alpha\beta}(\mathbf{u}) = u_{3|\alpha\beta} + b^\lambda_{\beta|\alpha}\,u_\lambda + b^\lambda_\beta\,u_{\lambda|\alpha} + b^\lambda_\alpha\,u_{\lambda|\beta} - b^\lambda_\alpha\,b_{\lambda\beta}\,u_3 \tag{2.12}$$

where

$$\text{(2.13)} \qquad \begin{cases} u_{\alpha|\beta} = u_{\alpha,\beta} - \Gamma^{\lambda}_{\alpha\beta}\, u_{\lambda} \\ b^{\lambda}_{\beta|\alpha} = b^{\lambda}_{\beta,\alpha} + \Gamma^{\lambda}_{\alpha\nu}\, b^{\nu}_{\beta} - \Gamma^{\nu}_{\beta\alpha}\, b^{\lambda}_{\nu} \\ u_{3|\alpha\beta} = u_{3,\alpha\beta} - \Gamma^{\lambda}_{\alpha\beta}\, u_{3,\lambda} \end{cases}$$

and Γ are the Christoffel symbols of S:

$$\text{(2.14)} \qquad \Gamma^{\alpha}_{\beta\gamma} = \Gamma^{\alpha}_{\gamma\beta} = \mathbf{a}^{\alpha} \cdot \mathbf{a}_{\gamma,\beta} = \mathbf{a}^{\alpha} \cdot \mathbf{a}_{\beta,\gamma} .$$

We then define the bilinear forms of membrane and flexion energy:

$$\text{(2.15)} \qquad a_0(\mathbf{u}, \mathbf{v}) = \int_S a_0^{\alpha\beta\eta\sigma}\, \gamma_{\eta\sigma}(\mathbf{u})\, \gamma_{\alpha\beta}(\mathbf{v})\, dS$$

$$\text{(2.16)} \qquad a_1(\mathbf{u}, \mathbf{v}) = \int_S a_1^{\alpha\beta\eta\sigma}\, \rho_{\eta\sigma}(\mathbf{u})\, \rho_{\alpha\beta}(\mathbf{v})\, dS$$

where the coefficients of a_0 and a_1 are elasticity coefficients satisfying the classical properties of symmetry and positivity

$$\text{(2.17)} \qquad a^{\alpha\beta\eta\sigma} = a^{\eta\sigma\alpha\beta} = a^{\alpha\beta\sigma\eta}$$

$$\text{(2.18)} \qquad a^{\alpha\beta\eta\sigma}\, \xi_{\alpha\beta}\, \xi_{\eta\sigma} \geqslant c \sum_{\alpha\beta} |\xi_{\alpha\beta}|^2 \quad \forall \xi_{\alpha\beta} \text{ symmetric} .$$

Moreover, the shell is supposed to be clamped by a part Γ_0 of the boundary, simply supported by another one Γ_1 and free by the remainder part. The kinematic boundary conditions to be prescribed are

$$\text{(2.19)} \qquad \begin{cases} \mathbf{u} = 0, \ \partial u_3 / \partial \nu & \text{on } \Gamma_0 \\ \mathbf{u} = 0 & \text{on } \Gamma_1 \end{cases}$$

where ν denotes the normal to the boundary. Let V be the space of the kinematically admissible displacements, defined by

$$\text{(2.20)} \qquad V = \{(v_1, v_2, v_3) \in H^1 \times H^1 \times H^2 \,;\, \mathbf{v} \text{ satisfy (2.19)}\}$$

The boundary conditions are supposed such that

$$\text{(2.21)} \qquad [a_0(\mathbf{v}, \mathbf{v}) + a_1(\mathbf{v}, \mathbf{v})]^{1/2}$$

is a norm on V equivalent to the classical one. This is the case if Ω is connected and Γ_0 is not empty [4], [5]. The shell problem is then:

$$\text{(2.22)} \qquad \begin{cases} \text{Find } \mathbf{u}^{\varepsilon} \in V \text{ such that} \\ \dfrac{1}{\varepsilon^2} a_0(\mathbf{u}^{\varepsilon}, \mathbf{v}) + a_1(\mathbf{u}^{\varepsilon}, \mathbf{v}) = \langle \mathbf{f}, \mathbf{v} \rangle_{V'V} \quad \forall \mathbf{v} \in V \end{cases}$$

where $\mathbf{f} \in V'$, $\varepsilon \in (0, \varepsilon_0)$ and the duality product is given by

$$\langle \mathbf{f}, \mathbf{v} \rangle_{V'V} = \int_S f^t v_t \, dS \,. \tag{2.23}$$

Clearly, by virtue of the hypothesis that (2.21) is a norm equivalent to that of V, the shell problem (2.22) has a unique solution for each fixed value of $\varepsilon \in (0, \varepsilon_0)$, in the framework of the Lax-Milgram theorem.

Our aim is to study the asymptotic behavior of $\mathbf{u}^\varepsilon$ as ε tends to zero and the corresponding Galerkin approximations.

Let V_h (with $h \searrow 0$) be a family of finite-dimensional subspaces of V such that V_h approaches V, i.e. such that

$$\forall \mathbf{v} \in V, \quad \lim_{h \searrow 0} \inf_{\mathbf{v}_h \in V_h} \| \mathbf{v} - \mathbf{v}_h \| = 0 \tag{2.24}$$

or, in other words:

$$\begin{cases} \forall \mathbf{v} \in V \quad \text{and} \quad h \searrow 0 \\ \text{there exists } \mathbf{v}_h \in V_h \text{ such that} \\ \mathbf{v}_h \in \mathbf{v} \text{ strongly in } V(h \searrow 0) \,. \end{cases} \tag{2.25}$$

We then consider the approximate problem associated with (2.22):

$$\begin{cases} \text{Find } \mathbf{u}_h^\varepsilon \in V_h \text{ such that} \\ \dfrac{1}{\varepsilon^2} a_0(\mathbf{u}_h^\varepsilon, \mathbf{v}) + a_1(\mathbf{u}_h^\varepsilon, \mathbf{v}) = \langle \mathbf{f}, \mathbf{v} \rangle_{V'V} \quad \forall \mathbf{v} \in V_h \,. \end{cases} \tag{2.26}$$

Moreover we shall admit that

$$\begin{cases} \forall \varepsilon > 0, \\ \mathbf{u}_h^\varepsilon \to \mathbf{u}^\varepsilon \text{ strongly in } V(h \searrow 0, \text{ fixed } \varepsilon) \,. \end{cases} \tag{2.27}$$

where $\mathbf{u}_h^\varepsilon$ and $\mathbf{u}^\varepsilon$ are respectively the solution of (2.26) and (2.22). We note that (2.27) holds true for a certain number of finite element approximations of the shell problem (see for instance [4], section II.1).

DEFINITION 2.1: *We say that V_h implies a robust approximation (2.26) of the problem (2.22) if the convergence (2.27) is uniform with respect to ε, i.e. if for given δ there exists γ such that*

$$\| \mathbf{u}_h^\varepsilon - \mathbf{u}^\varepsilon \|_V < \delta \text{ for } h \in (0, \gamma) \quad \text{and} \quad \varepsilon \in (0, \varepsilon_0) \tag{2.28}$$

We also say that the approximation V_h locks when it is not robust.

Remark 2.2: Property (2.28) ensures that an accurate approximation of the solution may be obtained with a sufficiently small mesh diameter h, independently of the thickness. Another possible definition of robutness involves uniformity of the convergence with respect to ε and to $\mathbf{f}$ (for $\mathbf{f}$ belonging to the unit ball of V', for instance), but we shall adopt in this paper the definition 2.1. ■

In practice if we have a locking approximation, we must fix γ in a suited form for each value of ε. In particular, changing the values of ε with a fixed mesh may spoil the quality of the approximation.

The following theorem will be the main tool for the study of locking in the next sections.

THEOREM 2.3: *Under the previous general hypotheses, let us consider the reiterated limits:*

$$\lim_{\varepsilon \searrow 0} \lim_{h \searrow 0} \mathbf{u}_h^\varepsilon \quad \text{strongly in } V \tag{2.29}$$

$$\lim_{h \searrow 0} \lim_{\varepsilon \searrow 0} \mathbf{u}_h^\varepsilon \quad \text{strongly in } V \tag{2.30}$$

and let us suppose that one the two hypotheses a) and b) hereafter is satisfied

a) the limits (2.29), (2.30) exist and are different,

b) the limit (2.29) exists but (2.30) does not.

Then the approximation V_h is not robust.

Remark 2.4: Let us point out that, denoting the solutions of (2.22) and (2.26) by $\mathbf{u}^\varepsilon$ and $\mathbf{u}_h^\varepsilon$ respectively, the limits

i) $\lim_{\varepsilon \to 0} \mathbf{u}^\varepsilon$ strongly in V

ii) $\lim_{\varepsilon \to 0} \mathbf{u}_h^\varepsilon$ strongly in V, for fixed h

always exist, as we shall prove later on in Theorem 3.2. In particular, from (2.27) and i) it follows that the reiterated limit (2.29) always exist, whereas (2.30) may exist or not.■

Proof of Theorem 2.3: It is a classical corollary of the theorem on uniform convergence of continuous functions. For the sake of completeness, let us recall theorem 66 of [20], vol. 1, p. 150: "Let E and F be two metric spaces, A a part of E and $f_0, f_1, ..., f_n ...$ a sequence of mappings of A into F converging uniformly to f. Let a be an accumulation point of A in E. If for each n, $f_n(x)$ has a limit when for x tending to a by points in A and if F is complete, then $f(x)$ has a limit for x tending to a by points in A and moreover"

$$\lim_{\substack{x \to a \\ x \in A}} f(x) = \lim_{n \to \infty} \left[\lim_{\substack{x \to a \\ x \in A}} f_h(x) \right]. \tag{2.31}$$

Let us apply this theorem taking $E = \mathbb{R}$, $F = V$ (which is a complete space), $x = \varepsilon$, $A = (0, \varepsilon_0)$ $f(x) = \mathbf{u}^\varepsilon$, $f_h(x) = \mathbf{u}_h^\varepsilon$ (with $h = h_n$, a sequence tending to 0 as n tends to infinity, $a = 0$. Let us suppose that the convergence $\mathbf{u}_h^\varepsilon \to \mathbf{u}^\varepsilon$ is uniform with respect to $\varepsilon \in (0, \varepsilon_0)$; then (2.31) holds true, taking the form

$$\lim_{\varepsilon \searrow 0} \mathbf{u}^\varepsilon = \lim_{h \searrow 0} \left[\lim_{\varepsilon \searrow 0} \mathbf{u}_h^\varepsilon \right] \tag{2.32}$$

which is in contraction with a) and b). ■

3. LIMIT PROCESSES AND CONSEQUENCES ON LOCKING

Let us define the closed subspace G of V formed by the pure bendings by:

$$\begin{aligned} G &= \{\mathbf{v} \in V ; a_0(\mathbf{v}, \mathbf{v}) = 0\} \\ &= \{\mathbf{v} \in V ; a_0(\mathbf{v}, \mathbf{w}) = 0 \quad \forall \mathbf{w} \in V\} \\ &= \{\mathbf{v} \in V ; \gamma_{\alpha\beta}(\mathbf{v}) = 0, \alpha, \beta = 1, 2\} \end{aligned} \tag{3.1}$$

We note that the three spaces appearing in the right side of (3.1) are the same. The equality of the first and the third ones follows from the definition of the form a_0 (2.15) and from the positivity of the coefficients (2.18). The equality of the first and the second spaces follows from the Cauchy-Schwarz inequality for the seminorm $a_0(\mathbf{v}, \mathbf{v})^{1/2}$:

$$|a_0(\mathbf{v}, \mathbf{w})| \leq a_0(\mathbf{v}, \mathbf{v})^{1/2} a_0(\mathbf{w}, \mathbf{w})^{1/2}. \tag{3.2}$$

The fact that G is closed follows immediately from (3.1) using for instance the second expression in the right side. Consequently G *is itself a Hilbert space* for the topology induced by that of V, and we may state the *limit problem for* $\varepsilon \to 0$:

$$\text{(3.3)} \qquad \begin{cases} \text{Find } \mathbf{u}^0 \in G \text{ such that} \\ a_1(\mathbf{u}^0, \mathbf{v}) = \langle \mathbf{f}, \mathbf{v} \rangle_{V'V} \quad \forall \mathbf{v} \in G \end{cases}$$

We note that, as a_0 vanishes on G, the left side of (3.3) is a form continuous and coercive on G, and consequently $\mathbf{u}^0$ exists and is unique in the classical framework of Lax-Milgram.

Remark 3.1: Let us consider the operators

$$\text{(3.4)} \qquad A_\varepsilon \in \mathcal{L}(V, V'), \quad \hat{A} \in \mathcal{L}(G, G')$$

defined by

$$\text{(3.5)} \qquad \langle A_\varepsilon \mathbf{u}, \mathbf{v} \rangle_{V'V} = \frac{1}{\varepsilon^2} a_0(\mathbf{u}, \mathbf{v}) + a_1(\mathbf{u}, \mathbf{v}) \quad \forall \mathbf{u}, \mathbf{v} \in V$$

$$\text{(3.6)} \qquad \langle \hat{A}\mathbf{u}, \mathbf{v} \rangle_{G'G} = a_1(\mathbf{u}, \mathbf{v}) \quad \forall \mathbf{u}, \mathbf{v} \in G .$$

It classically follows from the Lax-Milgram theorem that A_ε and $\hat{A}$ define isomorphisms of V onto V' and of G onto G' respectively. Moreover, V' may be decomposed as a direct sum:

$$\text{(3.7)} \qquad V' = G' \oplus G^p$$

where

$$G^p = \{\mathbf{f} \in V', \langle \mathbf{f}, \mathbf{v} \rangle_{V'V} = 0 \quad \forall \mathbf{v} \in G\}$$

is the polar set of G. We also note that the necessary and sufficient condition for $\mathbf{u}^0 \neq 0$ is that the component of $\mathbf{f}$ on G' does not vanish. ■

In the same way we define for each h:

$$\text{(3.8)} \qquad G_h = G \cap V_h = \{\mathbf{v} \in V_h \, ; \, a_0(\mathbf{v}, \mathbf{v}) = 0\} .$$

Let $\mathbf{u}_h^0$ be the solution of

$$\text{(3.9)} \qquad \begin{cases} \text{Find } \mathbf{u}_h^0 \in G_h \text{ such that} \\ a_1(\mathbf{u}_h^0, \mathbf{v}) = \langle \mathbf{f}, \mathbf{v} \rangle_{V'V} \quad \forall \mathbf{v} \in G_h . \end{cases}$$

We then have:

THEOREM 3.2: *Let* $\mathbf{u}^\varepsilon$, $\mathbf{u}_h^\varepsilon$, $\mathbf{u}^0$, $\mathbf{u}_h^0$ *be the solutions of (2.22), (2.26), (3.3) and (3.9) respectively. Then,*

$$\text{(3.10)} \qquad \mathbf{u}^\varepsilon \to \mathbf{u}^0 \quad \text{strongly in } V(\varepsilon \searrow 0)$$

$$\text{(3.11)} \qquad \mathbf{u}_h^\varepsilon \to \mathbf{u}_h^0 \text{ strongly in } V_h(\varepsilon \searrow 0, \text{ fixed } h)$$

Proof: It is classical as (3.10) and (3.11) are penalty limit processes. Let us prove for instance (3.11). Taking $\mathbf{v} = \mathbf{u}_h^\varepsilon$ in (2.26) it follows from the coerciveness of $a_0 + a_1$:

$$c\|\mathbf{u}_h^\varepsilon\|_V^2 \leqslant a_0(\mathbf{u}_h^\varepsilon, \mathbf{u}_h^\varepsilon) + a_1(\mathbf{u}_h^\varepsilon, \mathbf{u}_h^\varepsilon) \leqslant$$

(3.12)

$$\leqslant \frac{1}{\varepsilon^2} a_0(\mathbf{u}_h^\varepsilon, \mathbf{u}_h^\varepsilon) + a_1(\mathbf{u}_h^\varepsilon, \mathbf{u}_h^\varepsilon) = \langle \mathbf{f}, \mathbf{u}_h^\varepsilon \rangle_{V'V} \leqslant C\|\mathbf{u}_h^\varepsilon\|_V$$

for two non-vanishing constants c and C. We then see that the $\mathbf{u}_h^\varepsilon$ remain in a ball of the finite-dimensional space V_h. After extraction of a subsequence (in fact it is the whole sequence because we shall see later that the limit is unique)

$$\mathbf{u}_h^\varepsilon \to \mathbf{u}^* \text{ weakly and strongly in } V_h (\varepsilon \searrow 0, \text{ fixed } h) . \tag{3.13}$$

It follows from (3.12) that

$$a_0(\mathbf{u}_h^\varepsilon, \mathbf{u}_h^\varepsilon)^{1/2} \leqslant K\varepsilon . \tag{3.14}$$

On the other hand, for any fixed $\mathbf{v} \in V_h$, we have from (3.13):

$$a_0(\mathbf{u}_h^\varepsilon, \mathbf{v}) \to a_0(\mathbf{u}^*, \mathbf{v}) \quad (\varepsilon \searrow 0, \text{ fixed } h) , \tag{3.15}$$

and, using (3.14) and an estimate analogous to (3.2) we see that the left side of (3.15) converges to zero in modulus, and consequently $a_0(\mathbf{u}^*, \mathbf{v}) = 0$. Taking $\mathbf{v} = \mathbf{u}^*$ we see that $\mathbf{u}^* \in G_h$. On the other hand, taking in (2.26) $\mathbf{v} \in G_h$ we have:

$$a_1(\mathbf{u}_h^\varepsilon, \mathbf{v}) = \langle \mathbf{f}, \mathbf{v} \rangle_{V'V} \quad \forall \mathbf{v} \in G_h . \tag{3.16}$$

and letting $\varepsilon \searrow 0$, we have, according to (3.13):

$$a_1(\mathbf{u}^*, \mathbf{v}) = \langle \mathbf{f}, \mathbf{v} \rangle_{V'V} \quad \forall \mathbf{v} \in G_h . \tag{3.17}$$

As we saw that $\mathbf{u}^* \in G_h$, $\mathbf{u}^* = \mathbf{u}_h^0$ is the only solution of (3.9) and (3.11) is proven.

The proof of (3.10) follows exactly the same steps, showing the weak convergence in V. The strong convergence in V needs and ulterior reasoning. As we pointed out before, the proof is classical, and may be seen for instance in [6], Theorem 1. ■

The result (3.10) constitutes the fundamental property of thin shells. When the thickness tends to zero, the solutions converge to a solution which is an inextensional displacement, i.e. a pure bending. This property is meaningfull in the case when the shell is "*non-inhibited*", i.e. S admits non zero pure bendings, or

$$G \neq \{0\} . \tag{3.18}$$

In the *inhibited* case, i.e. $G = \{0\}$, (3.10) always hold true, but evidently $\mathbf{u}^0 = 0$. In order to have a better description of the asymptotic behavior of $\mathbf{u}^\varepsilon$ we write $\mathbf{u}^\varepsilon = \varepsilon^2 \mathbf{v}^\varepsilon$ and we study the limit behavior of $\mathbf{v}^\varepsilon$. This asymptotic process, which has nothing to do with the membrane locking may be seen in [15] or [16], [17].

According to (3.11) an analogous behavior holds for the approximate problem in the space V_h. *The membrane locking occurs when G_h does not approach G.* More precisely:

PROPOSITION 3.3: *Let us admit the general hypotheses of this paper, in particular V_h approaches V, (see (2.25)). Moreover, let us assume that the subspaces $G_h = G \cap V_h$ defined in (3.8) do not approach G, defined in (3.1) (in other words, there exists at least a non-zero element $\hat{\mathbf{v}}$ of G which cannot be approached in the form (2.25), with G and G_h instead of V and V_h, respectively).*

Then the approximation of problem (2.22) by V_h is not robust (locking holds at least for certain $\mathbf{f}$, *for instance for* $\mathbf{f} = \hat{A}\hat{\mathbf{v}}$ *where* $\hat{A}$ *denotes the operator defined in (3.6)).*

Proof: We consider problems (2.22) and (2.26) with $\mathbf{f} = \hat{A}\hat{\mathbf{v}}$. We are showing that we then are in the hypotheses of theorem 2.3. From (2.27) we see that the limit $h \searrow 0$ of $\mathbf{u}_h^\varepsilon$ exists and is $\mathbf{u}^\varepsilon$. Next, the limit $\varepsilon \searrow 0$ of $\mathbf{u}^\varepsilon$ exists by (3.10) and is equal to $\mathbf{u}^0$, which is in fact $\hat{\mathbf{v}}$ for the considered force $\mathbf{f}$ (see (3.3) and (3.6) if necessary). It then follows that the reiterated limit (2.29) exists and is equal to $\hat{\mathbf{v}}$. On the other hand, the reiterated limit (2.30) becomes by virtue of (3.11)

$$\lim_{h \searrow 0} \mathbf{u}_h^0 \quad \text{strongly in } V \tag{3.19}$$

but $\mathbf{u}_h^0 \in G_h \subset G$, and the convergence in (3.19) is in fact "strongly in G". This limit may exist or not exist, but in any case by hypothesis, it is not equal to $\hat{\mathbf{v}}$, and theorem 2.3 applies. ■

Remark 3.4: Locking holds in particular when $G \neq \{0\}$ but $G_h = G \cap V_h = \{0\}$ for any h. In that case we have a total locking, for any $\mathbf{f}$ with non-zero component in G'. ■

Remark 3.5: We shall see in the next sections examples where $\mathbf{v} \in G_h$ implies $v_3 = 0$, but G contain elements with non-zero third component. Clearly in that case the G_h do not approach G (see (2.25) with G and G_h instead of V and V_h, respectively) and locking holds. ■

4. ANY PIECEWISE POLYNOMIAL INTERNAL APPROXIMATION IS NECESSARILY NOT ROBUST (OR LOCKS)

In this section we are proving that any finite element internal approximation of the shell problem such that the elements of V_h are in each triangle of the mesh polynomial functions (i.e. practically any finite element method) locks for certain shapes of the middle surface. Clearly we may wonder if there is no locking for other surfaces. This is the reason why we first give some heuristic reasons showing that locking is probably a generic phenomenon, holding for almost any surface, with a very few exceptions.

As we saw in proposition 3.3, locking appears when the spaces $G_h = G \cap V_h$ do not approach G where

$$G_h = \{\mathbf{v} \in V_h \,;\, \gamma_{\alpha\beta}(\mathbf{v}) = 0, \quad \alpha, \beta = 1, 2\} \tag{4.1}$$

In order to get an intuitive idea of the nature of this problem, let us consider to simplify and fix ideas, the case when the $b_{\alpha\beta}$ are constant and the Christoffel symbols vanish. The constraints appearing in (4.1) are then:

$$\begin{cases} \gamma_{11}(\mathbf{v}) \equiv \partial_1 v_1 - b_{11} v_3 = 0 \\ \gamma_{22}(\mathbf{v}) \equiv \partial_2 v_2 - b_{22} v_3 = 0 \\ \gamma_{12}(\mathbf{v}) \equiv \frac{1}{2}(\partial_2 v_1 + \partial_1 v_2) - b_{12} v_3 = 0 \end{cases} \tag{4.2}$$

Let us admit that one of the coefficients b_{11} and b_{22} does not vanish. This condition is generally satisfied, and certainly it does if the surface is either elliptic or parabolic. Let $b_{11} \neq 0$. The first condition (4.2) shows that

$$\mathbf{v} \in G_h \Rightarrow v_3 = \frac{1}{b_{11}} \partial_1 v_1 \tag{4.3}$$

Let us consider the restriction of (4.3) to a triangle of the mesh. Then, as v_1 is a polynomial of some degree m, v_3 is necessarily a polynomial of degree $m - 1$. This is perfectly incoherent with the fact that the components v_α ($\alpha = 1, 2$) belong to H^1 but $v_3 \in H^2$: any finite element scheme classically used in shell theory (cf. [4] for instance) uses polynomials of higher order in the discretization of v_3 than in that of v_1, v_2. In these conditions, the convergence of the approximation is seriously compromised.

It should be noticed that the above reasoning is very close to that of [6], theorem 4, where it is shown that in the case of a circular arch, there is a robust non-classical approximation by finite elements where v_α

($\alpha = 1, 2$) and v_3 by polynomials of orders 4 and 3 respectively But we should not conclude that discretizing v_3 by polynomials of lower order than v_α is a general way for avoiding locking We are showing that any internal approximation which is piecewise polynomial locks for certain surfaces

Our proof is mainly based on Remarks 3 4 and 3 5 For certain specific surfaces, we shall show that $\mathbf{v} \in G_h$ implies either $\mathbf{v} = 0$ or $v_3 = 0$ The cases considered are the straight helicoid, and the hyperbolic and elliptic paraboloids Clearly the applications to locking only concern non-inhibited surfaces, an this implies some conditions on the fixation of the boundaries In particular, a part of them (or even the whole) must be free Examples may be seen in [18] and [8], but we shall see later (section 6) an example of non-inhibited hyperbolic paraboloid But the following proofs are essentially very simple and are not concerned with the boundary conditions According to (4 1), taking $\mathbf{v} \in G_h$ and taking the restriction to an element of the mesh, it is sufficient to show that if each component of $\mathbf{v}$ is a polynomial then

$$\gamma_{\alpha\beta}(\mathbf{v}) = 0 \ (\alpha, \beta = 1, 2) \Rightarrow \mathbf{v} = 0 \ (\text{or merely } v_3 = 0) \tag{4 4}$$

Case of the hyperbolic paraboloid

It is the surface defined by (notation of sect 2)

$$\boldsymbol{\varphi}(y^1, y^2) = (y^1, y^2, y^1 y^2) \tag{4 5}$$

We obtain easily

$$\mathbf{a}_1 = (1, 0, y^2), \quad \mathbf{a}_2 = (0, 1, y^1), \quad \mathbf{a}_3 = a^{-1/2}(-y^2, -y^1, 1) \tag{4 6}$$

where

$$a = 1 + (y^1)^2 + (y^2)^2 \tag{4 7}$$

Moreover,

$$b_{11} = b_{22} = 0, \quad b_{12} = a^{-1/2} \tag{4 8}$$

$$\begin{cases} \mathbf{a}^1 = a^{-1}(1 + (y^1)^2, -y^1 y^2, y^2), \\ \mathbf{a}^2 = a^{-1}(-y^1 y^2, 1 + (y^2)^2, y^1), \\ \mathbf{a}^3 = \mathbf{a}_3 \end{cases} \tag{4 9}$$

$$\Gamma^\alpha_{11} = \Gamma^\alpha_{22} = 0, \quad \Gamma^1_{12} = a^{-1} y^2, \quad \Gamma^2_{12} = a^{-1} y^1 \tag{4 10}$$

The system (4 4) becomes

$$\begin{cases} \partial_1 u_1 = 0 \\ \partial_2 u_2 = 0 \\ \partial_2 u_1 + \partial_1 u_2 = 2\, a^{-1/2} u_3 + 2\, a^{-1} y^2 u_1 + 2\, a^{-1} y^1 u_2 \end{cases} \tag{4 11}$$

and consequently

$$2\, a^{1/2} u_3 = a(\partial_2 u_1 + \partial_1 u_2) - 2\, y^2 u_1 - 2\, y^1 u_2 \tag{4 12}$$

which on account of (4 7) and of the fact that u_i are polynomials, implies $u_3 = 0$ As we mentioned above, this implies locking in the context of Remark 3 5 Moreover, we may show that $u_1 = u_2 = 0$ To this end, we note

that whatever the considered triangle be, polynomials are analytic functions, and it is sufficient to check that they vanish in a neighbourhood of the origin. Equation (4.12) with $u_3 = 0$ and (4.11) becomes

$$[1 + (y^1)^2 + (y^2)^2]\,[u_1'(y^2) + u_2'(y^1)] = 2\,y^2\,u_1(y^2) + 2\,y^1\,u_2(y^1) \tag{4.13}$$

where' denotes differentiation. For $y^1 = 0$ this gives

$$[1 + (y^2)^2]\,[u_1'(y^2) + const.] = 2\,y^2\,u_1(y^2) \tag{4.14}$$

and it is easily seen that u_1 is of the form

$$u_1 = c[1 + (y^2)^2]\,. \tag{4.15}$$

Obviously, $u_2(y^1)$ has an analogous expression and replacing them in (4.13) we see that u_1 and u_2 vanish identically. Finally we are in the context of Remark 3.4 and we have *total locking.* ■

Case of the elliptic paraboloid

The calculations are essentially analogous to those of the previous case. We have:

$$\varphi(y^1, y^2) = \left(y^1, y^2, \frac{1}{2}\,[(y^1)^2 + (y^2)^2]\right) \tag{4.16}$$

$$\mathbf{a}_1 = (1, 0, y^1), \quad \mathbf{a}_2 = (0, 1, y^2), \quad \mathbf{a}_3 = a^{-1/2}(-y^1, -y^2, 1) \tag{4.17}$$

with

$$a = 1 + (y^1)^2 + (y^2)^2 \tag{4.18}$$

$$b_{11} = b_{22} = a^{-1/2}, \quad b_{12} = 0 \tag{4.19}$$

$$\Gamma^1_{11} = \Gamma^1_{22} = a^{-1}\,y^1, \quad \Gamma^2_{11} = \Gamma^2_{22} = a^{-1}\,y^2, \quad \Gamma^\alpha_{12} = 0 \tag{4.20}$$

and the system (4.4) becomes

$$\begin{cases} \partial_1 u_1 = \partial_2 u_2 = \dfrac{y^1}{a}\,u_1 + \dfrac{y^2}{a}\,u_2 + \dfrac{1}{a^{1/2}}\,u_3 \\ \partial_2 u_1 + \partial_1 u_2 = 0 \end{cases} \tag{4.21}$$

Multiplying the first equation (4.21) by a, we get

$$a\partial_1 u_1 = a\partial_2 u_2 = y^1 u_1 + y^2 u_2 + a^{1/2} u_3 \tag{4.22}$$

which, on account of (4.18) implies $u_3 = 0$ as the u_i are polynomials. It is also possible in this case to prove that $u_1 = u_2 = 0$, but the proof is more involved than in the previous examples. We shall not give it here, but in any case *we have locking* in the framework or Remark 3.5. ■

Case of the straight helicoid

In that case, we have

$$\varphi(y^1, y^2) = \varphi(\theta, r) = (r\cos\theta, r\sin\theta, k\theta) \tag{4.22}$$

$$\begin{cases} \mathbf{a}_1 = (-r\sin\theta, r\cos\theta, k)\,, \\ \mathbf{a}_2 = (\cos\theta, \sin\theta, 0)\,, \\ \mathbf{a}_3 = a^{-1/2}(-k\sin\theta, k\cos\theta, -r) \end{cases} \tag{4.23}$$

where

(4 24) $$a = r^2 + k^2$$

Moreover

(4 25) $$b_{11} = b_{22} = 0, \quad b_{12} = ka^{-1/2}$$

(4 26) $$\Gamma^{\alpha}_{22} = \Gamma^{1}_{11} = \Gamma^{2}_{12} = 0, \quad \Gamma^{2}_{11} = -r, \quad \Gamma^{1}_{12} = a^{-1} r$$

(4 27) $$\begin{cases} \partial_1 u_1 = -ru_2 \\ \partial_2 u_2 = 0 \\ \partial_2 u_1 + \partial_1 u_2 = 2a^{-1} r u_1 + 2a^{-1/2} k u_3 \end{cases}$$

and from the third equation of (4 27) we get

(4 28) $$2ka^{1/2} u_3 = a(\partial_2 u_1 + \partial_1 u_2) - 2ru_1$$

It then follows from (4 24) that $u_3 = 0$, and *we have locking again* in the framework of Remark 3 5

The previous considerations show the very general character of membrane locking in non-inhibited shells Moreover, it appears that membrane locking is concerned with the specific local structure of the *equations,* without taking into account the boundary conditions, this situation is in contrast with the classical locking of H^1 finite element approximations in incompressible fluid mechanics, where $\mathbf{v} \in G_h$ implies $\mathbf{v} = 0$ only on account of boundary conditions and interaction between the various finite elements

Remark 4 1 Obviously a plate is a particular case of shell When shell finite elements are used in plates, membrane locking do not appear This is easily seen from system (4 2) in the case of a plate, $b_{\alpha\beta} = 0$, and (4 2) shows that the elements of G are such that (v_1, v_2) is a rigid displacement in the plane (usually vanishing according to the boundary conditions) whereas v_3 is arbitrary G_k has an analogous definition, and G_k approaches G provided that the approximation of V by V_h is independent for the three components as obviously happens for any usual finite element approximation ■

5. LOCKING IN THE NON-CONFORMING DKT APPROXIMATION

In this section we prove that the previous considerations on membrane locking also hold true for the widely used DKT (= "Discrete Kirchhoff Triangle") which is non-conforming (i e V_h is non contained in V) This approximation is described in detail in [4] chap II 2

In principle the DKT approximation involves displacements and rotations Nevertheless, there exists an equivalent formulation involving only displacements, after eliminating the rotations (cf [4] formula (2 25), p 118) In fact, this formulation is exactly analogous to (2 26) with a certain space V_h not contained in V, but such that $\mathbf{v} \in V_h$ implies that v_t is a polynomial in each finite element We then define G_h by

(5 1) $$G_h = \{\mathbf{v} \in V_h, \quad \gamma_{\alpha\beta}(\mathbf{v}) = 0, \quad \alpha = 1, 2\}$$

and we obtain the convergence (3 11) in V_h exactly as in theorem 3 2 Moreover, theorem 2 3 holds true, provided that the strong convergence in V be replaced by convergence in a space containing V and V_h, for instance $(L^2(\Omega))^3$ Let us also remark that the convergence (2 27) also holds true in this space (cf [4] theorem 2 2 6, p 122), we recall in this concern that the hypothesis that the shell is clamped all along its boundary may be

weakened according the remarks of [4] p 120 The definitions of "V_h approaches" and "G_h approaches G" are analogous to (2 24) and (2 25) but the norms are again in $(L^2(\Omega))^3$ In these conditions, Proposition 3 3 and Remarks 3 4 and 3 5 hold true, as well as the consideration of section 4 and the locking of the DKT approximation follows

6. NUMERICAL EXPERIMENTS

In this section we display some numerical results concerning locking phenomenon, we compare the performance of two finite element methods (conforming and non-conforming) and the behaviour with respect to different reduced integration schemes

We consider the hyperbolic paraboloid problem (see the *fig 1* for the physical data of the shell) The thickness of the shell is $2\,\varepsilon = 10^{-n}$, with $n = 1, 2, 3, 4, 5$, we remark that for $n = 4, 5$ we have really a "very" thin shell, perhaps without physical interpretation

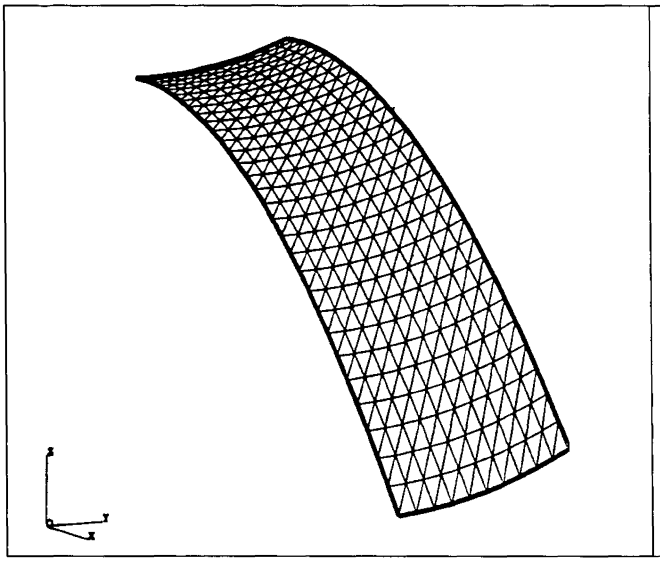

$$\bar{\Omega} = [0, 3] \times [0, 1]$$
$$\vec{\varphi}(y^1, y^2) = (y^1, y^2, \alpha((y^1)^2 - (y^2)^2))$$
$$\alpha = 0\,2$$
$$E = 2{,}85*10^4$$
$$\nu = 0\,3$$
$$\vec{\mathbf{f}} = 8\,\varepsilon^3\,\vec{\mathbf{a}}_3$$

Boundary conditions:

$$\vec{\mathbf{u}} = \vec{\mathbf{0}} \text{ on } (0, 0)(0, 1)$$
$$\frac{\partial u_3}{\partial \nu} = 0 \text{ on } (0, 0)(0, 1)$$

$\vec{\mathbf{u}}$ symmetric on (0, 0) (3, 0)
(corresponding to a physical problem
on $[0, 3] \times [-1, +1]$
with symmetric loading)

Figure 1. — Hyperbolic paraboloid.

We consider in the following two different finite element methods

- the Ganev-Argyris' method this is a well known conforming method which uses the P_4 -Ganev triangle for the approximation of the tangent components of the displacement, and the P_5 -Argyris triangle for the normal component, there are 15 + 15 + 21 degrees of freedom in each triangle,
- the Sander's delinquent method this is a non-conforming method which uses the P_2 -Lagrange-edge triangle for the tangent components and the Sander's delinquent triangle for the normal component now there are 6 + 6 + 12 degrees of freedom in each triangle

The definition of these finite elements is described in figures 2 and 3 using the classic notation of [7]

For the approximation properties of the above-mentioned elements, we refer to [4] (p 110 and 114) Here, we recall the main results

- the Ganev-Argyris' method is a high-degree approximation because the order of convergence is $O(h^4)$ (h is the diameter of the triangulation), this order is preserved if a reduced integration scheme exact for the polynomials of degree 6 is used,
- the order of convergence of the Sander's methods is $O(h^2)$ and the integration scheme have to be exact for the polynomials of degree 4

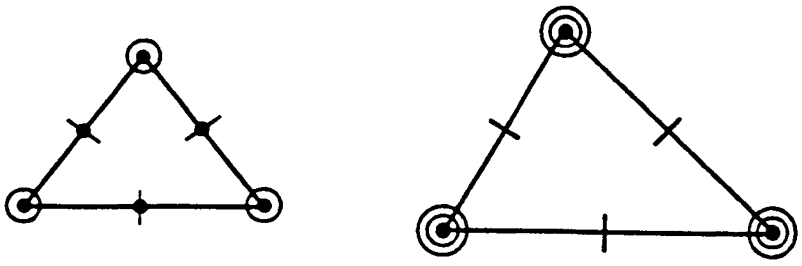

Ganev triangle

$$P_{KG} = P_4(K)\ (dim\ P_{KG} = 15)$$
$$\Sigma_{KG} = \{p(a_i), p_{,1}(a_i), p_{,2}(a_i), p(b_i), p_{,n_i}(b_i) : i = 1, 2, 3\}$$

Argyris triangle

$$P_{KA} = P_5(K)\ (dim\ P_{KA} = 21)$$
$$\Sigma_{KA} = \{p(a_i), p_{,1}(a_i), p_{,2}(a_i), p_{,11}(a_i), p_{,12}(a_i), p_{22}(a_i), p_{,n_i}(b_i) : i = 1, 2, 3\}$$

Figure 2. — The Ganev-Argyris method.

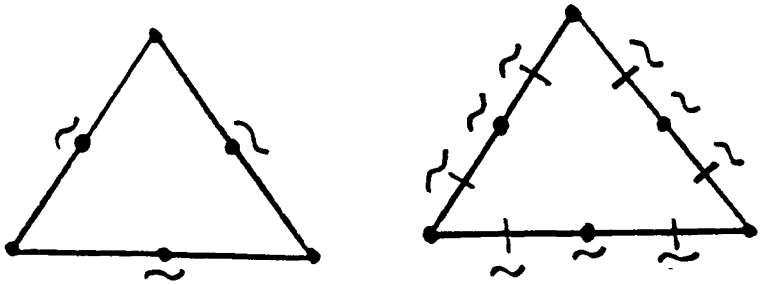

P_2-Lagrange - edge triangle

$$P_{K\bar{2}} = P_2(K)\ (dim\ P_{K\bar{2}} = 6)$$
$$\Sigma_{K\bar{2}} = \left\{ p(a_i), \frac{1}{l_i}\int_{K_i} p\, d\gamma : i = 1, 2, 3 \right\}$$

Sander's delinquent triangle

$$P_{KS} = P'_3(K) \oplus (\lambda_1 \lambda_2 \lambda_3 \lambda_i)_{i=1,2,3}\ (dim\ P_{KS} = 12)$$
$$\Sigma_{KS} = \left\{ p(a_i), \frac{1}{l_i}\int_{K_i} p\, d\gamma, \frac{1}{l_i}\int_{K_i} \lambda_{i-1} p_{,n_i}\, d\gamma, \frac{1}{l_i}\int_{K_i} \lambda_{i+1} p_{,n_i}\, d\gamma : i = 1, 2, 3 \right\}$$

Figure 3. — The Sander's delinquent method

For each method we have made use of 6 integration schemes (see [12]):

1. Scheme exact for P_2 with 3 nodes;
2. Scheme exact for P_3 with 7 nodes;
3. Scheme exact for P_4 with 6 nodes;
4. Scheme exact for P_6 with 12 nodes;
5. Scheme exact for P_8 with 16 nodes;
6. Scheme exact for P_9 with 22 nodes;

Remark 6.1: Actually, we tested 13 reduced integration schemes, but the results obtained were similar to the above mentioned ones to which we reduce our presentation. ■

Clearly a scheme is optimal when it assures the convergence of the finite element method with a minimal number of nodes; for the Ganev-Argyris' method the optimal scheme is 4 and for the Sander's method is 3. We note that for the low precision schemes the order of convergence of the method is not assured (it is the case of 1 and 2 for the Sander's method and 2 and 3 for the Ganev-Argyris' method) or even the matrix of the discrete problem may be singular (it is the case of 1 for Ganev-Argyris). These schemes may be considered as "reduced integration schemes".

The meshes follow the topological disposition of figure 1. The step h is reduced in the usual way. Computation were performed on a HP/Apollo computer using the MODULEF Code.

The results are displayed for the normal displacement u_3 at the point $A = \bar{\varphi}(3, 1)$. The results obtained for the different meshes, integration schemes, thickness and finite elements methods are summarized in the figure 4a and 4b for the value $\alpha = 0.2$ of the parameter (see *fig. 1*).

Remark 6.2: The same problem was also considered for a different geometry, $\alpha = 0.1$ (see *fig. 1*), but the main trends of the numerical results are the same as for $\alpha = 0.2$.

In figures 5c, d, e, f we show (in logarithmic scale) the relation between the thickness and $u_3(A)$ for two values of h (attention to the y-scale).

F.E.M.	Coarse mesh	Fine mesh
Ganev - Argyris	*h = 1/2*	*h = 1/10*
Sander	*h = 1/4*	*h = 1/123*

Figures 5c, d, e, f.

In figure 6(g-j) we show the convergence of the methods for two values of the thickness when dim $V_h \to \infty$ (we recall that dim $V_h \to \infty$ is equivalent to $h \to 0$).

We recall that membrane locking amounts to non-uniformity (with respect to ε) of the convergence $h \searrow 0$. Equivalently, as our example is one of total locking (see (3.11), Remark 3.4 and section 4) the limit of $\mathbf{u}_h^\varepsilon$ as $\varepsilon \searrow 0$ with fixed h is zero. All these features are apparent in the previous numerical results.

Our computations were roughly done up to the reasonable capability of an Apollo station. It then appears that with the Ganev-Argyris scheme locking is only evident with very small ε : the lack of convergence only appears in our example for $\varepsilon \leqslant 10^{-3}$ (we recall that 2ε = thickness). On the contrary, for the Sander method the lacking is clear (attention must be payed to the y-scale in *fig. 5*). Even for $\varepsilon = 10^{-2}$ the convergence is hard and for $\varepsilon = 10^{-3}$ the results are completely different from the Ganev-Argyris ones.

The better behavior of the Ganev-Argyris scheme may be understood as a better ability of the high degree polynomials for approximating the very peculiar functions of the limit space G. Equivalently, the rate of convergence in h^4 (instead of h^2 for the Sander scheme) shows the higher efficacity of the $h \searrow 0$ process on convergence. See also [14] in this concern.

Thickness	$\varepsilon = 10^{-1}$	$h = 1$	$h = 1/2$	$h = 1/4$	$h = 1/6$	$h = 1/8$	$h = 1/10$
Exact for P-3	(7 nodes)	4.203958494E-3	3.945799620E-3	4.022844204E-3	4.018861022E-3	4.001460078E-3	3.985156914E-3
Exact for P-4	(6 nodes)	2.456312449E-3	2.433293064E-3	2.433551941E-3	2.433945664E-3	2.434139778E-3	2.434248111E-3
Exact for P-6	(12 nodes)	2.421042009E-3	2.431039395E-3	2.433061242E-3	2.433672158E-3	2.433957386E-3	2.434116009E-3
Exact for P-8	(16 nodes)	2.420626365E-3	2.431033807E-3	2.433061032E-3	2.433672109E-3	2.433957367E-3	2.434116001E-3
Exact for P-9	(22 nodes)	2.420633738E-3	2.431033308E-3	2.433060900E-3	2.433672049E-3	2.433957334E-3	2.434115979E-3
Thickness	$\varepsilon = 10^{-2}$	$h = 1$	$h = 1/2$	$h = 1/4$	$h = 1/6$	$h = 1/8$	$h = 1/10$
Exact for P-3	(7 nodes)	2.440116277E-3	1.875194248E-3	1.586960520E-3	1.529566461E-3	1.503451179E-3	1.486329503E-3
Exact for P-4	(6 nodes)	1.148895782E-3	1.192021252E-3	1.187608280E-3	1.186966740E-3	1.186925097E-3	1.186957557E-3
Exact for P-6	(12 nodes)	9.213010749E-4	1.170645022E-3	1.185854344E-3	1.186498792E-3	1.186701133E-3	1.186814773E-3
Exact for P-8	(16 nodes)	9.197055719E-4	1.170744645E-3	1.185846196E-3	1.186497892E-3	1.186700898E-3	1.186814677E-3
Exact for P-9	(22 nodes)	9.189212547E-4	1.170724654E-3	1.185846018E-3	1.186497799E-3	1.186700845E-3	1.186814644E-3
Thickness	$\varepsilon = 10^{-3}$	$h = 1$	$h = 1/2$	$h = 1/4$	$h = 1/6$	$h = 1/8$	$h = 1/10$
Exact for P-3	(7 nodes)	2.409149928E-3	1.722327076E-3	1.247897619E-3	1.130169866E-3	1.080134151E-3	1.053471227E-3
Exact for P-4	(6 nodes)	5.511134814E-4	8.169386324E-4	8.896640710E-4	8.961747998E-4	8.961588082E-4	8.957948970E-4
Exact for P-6	(12 nodes)	2.691407585E-4	6.676128557E-4	8.694456362E-4	8.902733914E-4	8.938437241E-4	8.947188991E-4
Exact for P-8	(16 nodes)	2.624204068E-4	6.680589212E-4	8.698656791E-4	8.902848274E-4	8.938310789E-4	8.947132894E-4
Exact for P-9	(22 nodes)	2.613995673E-4	6.674364174E-4	8.697949969E-4	8.902793826E-4	8.938306879E-4	8.947131909E-4
Thickness	$\varepsilon = 10^{-4}$	$h = 1$	$h = 1/2$	$h = 1/4$	$h = 1/6$	$h = 1/8$	$h = 1/10$
Exact for P-3	(7 nodes)	2.408838375E-3	1.718420170E-3	1.214056131E-3	1.064992396E-3	9.949873520E-4	9.553395842E-4
Exact for P-4	(6 nodes)	3.298863403E-4	3.821151008E-4	6.591563647E-4	7.460556037E-4	7.707708931E-4	7.789165612E-4
Exact for P-6	(12 nodes)	1.667651552E-5	1.971934910E-4	5.652402917E-4	7.107755410E-4	7.536027471E-4	7.691043852E-4
Exact for P-8	(16 nodes)	1.497612732E-5	1.948803217E-4	5.592687064E-4	7.089154601E-4	7.533233192E-4	7.692033088E-4
Exact for P-9	(22 nodes)	1.486229021E-5	1.947419370E-4	5.589554733E-4	7.087777145E-4	7.532798423E-4	7.691858912E-4
Thickness	$\varepsilon = 10^{-5}$	$h = 1$	$h = 1/2$	$h = 1/4$	$h = 1/6$	$h = 1/8$	$h = 1/10$
Exact for P-3	(7 nodes)	2.408970700E-3	1.718413875E-3	1.213644498E-3	1.062309629E-3	9.865819032E-4	9.412020679E-4
Exact for P-4	(6 nodes)	1.436911671E-4	4.866688656E-5	2.731928769E-4	4.777639071E-4	5.991388488E-4	6.593080579E-4
Exact for P-6	(12 nodes)	2.262682624E-6	1.308601054E-5	1.813510247E-4	3.832255891E-4	5.335645480E-4	6.181002194E-4
Exact for P-8	(16 nodes)	2.188592017E-6	1.221459225E-5	1.755449559E-4	3.731466106E-4	5.259278511E-4	6.133233331E-4
Exact for P-9	(22 nodes)	2.187287960E-6	1.218539031E-5	1.753719380E-4	3.729232615E-4	5.257503704E-4	6.131126632E-4

Figure 4a. — Ganev-Argyris

Thickness ε = 10^-1	*h = 1/2*	*h = 1/4*	*h = 1/6*	*h = 1/8*	*h = 1/10*
Exact for P-2 (3 nodes)	2.604991677E-3	2.488607496E-3	2.455951795E-3	2.445000073E-3	2.440402073E-3
Exact for P-3 (7 nodes)	2.306362717E-3	2.425501070E-3	2.432592325E-3	2.433789026E-3	2.434127369E-3
Exact for P-4 (6 nodes)	2.337713829E-3	2.428090433E-3	2.433187100E-3	2.434020027E-3	2.434249062E-3
Exact for P-6 (12 nodes)	2.337514121E-3	2.428085197E-3	2.433186366E-3	2.434019809E-3	2.434248964E-3
Exact for P-8 (16 nodes)	2.337514936E-3	2.428085213E-3	2.433186368E-3	2.434019807E-3	2.434248967E-3
Exact for P-9 (22 nodes)	2.337514275E-3	2.428085073E-3	2.433186309E-3	2.434019776E-3	2.434248936E-3
Thickness ε = 10^-2	*h = 1/2*	*h = 1/4*	*h = 1/6*	*h = 1/8*	*h = 1/10*
Exact for P-2 (3 nodes)	4.006403018E-4	1.034478714E-3	1.165957105E-3	1.189041148E-3	1.192921624E-3
Exact for P-3 (7 nodes)	2.557792631E-4	8.552603124E-4	1.094175541E-3	1.155219754E-3	1.173755289E-3
Exact for P-4 (6 nodes)	2.999151400E-4	9.208149792E-4	1.117549289E-3	1.163683370E-3	1.177384480E-3
Exact for P-6 (12 nodes)	2.946492212E-4	9.202305087E-4	1.117480942E-3	1.163669553E-3	1.177380464E-3
Exact for P-8 (16 nodes)	2.946732281E-4	9.202313689E-4	1.117481054E-3	1.163669586E-3	1.177380474E-3
Exact for P-9 (22 nodes)	2.946724486E-4	9.202308294E-4	1.117480847E-3	1.163669497E-3	1.177380428E-3
Thickness ε = 10^-3	*h = 1/2*	*h = 1/4*	*h = 1/6*	*h = 1/8*	*h = 1/10*
Exact for P-2 (3 nodes)	3.425484973E-5	6.535143521E-5	1.935798087E-4	3.855129820E-4	5.641766002E-4
Exact for P-3 (7 nodes)	7.236455110E-6	4.142733068E-5	1.328236774E-4	2.740887643E-4	4.350489440E-4
Exact for P-4 (6 nodes)	9.991200830E-6	5.197426694E-5	1.570063645E-4	3.200204855E-4	4.934630723E-4
Exact for P-6 (12 nodes)	7.104299501E-6	4.915126875E-5	1.540205174E-4	3.180255053E-4	4.925310702E-4
Exact for P-8 (16 nodes)	7.063661296E-6	4.916514927E-5	1.540368915E-4	3.180350765E-4	4.925346880E-4
Exact for P-9 (22 nodes)	7.063132749E-6	4.916494355E-5	1.540365947E-4	3.180346490E-4	4.925342162E-4
Thickness ε = 10^-4	*h = 1/2*	*h = 1/4*	*h = 1/6*	*h = 1/8*	*h = 1/10*
Exact for P-2 (3 nodes)	2.944222034E-5	1.518837151E-5	1.349536986E-5	1.653739757E-5	2.461805902E-5
Exact for P-3 (7 nodes)	3.108962517E-6	1.911301184E-6	3.061244999E-6	6.711542106E-6	1.363281000E-5
Exact for P-4 (6 nodes)	1.716207731E-6	3.017522135E-6	5.362611729E-6	1.034847966E-5	1.896680004E-5
Exact for P-6 (12 nodes)	1.013441921E-7	1.008553067E-6	3.596620896E-6	8.667831467E-6	1.720887586E-5
Exact for P-8 (16 nodes)	9.631274995E-8	9.834400428E-7	3.576981011E-6	8.666838135E-6	1.721663575E-5
Exact for P-9 (22 nodes)	9.624801170E-8	9.833584537E-7	3.576930653E-6	8.666794753E-6	1.721657990E-5
Thickness ε = 10^-5	*h = 1/2*	*h = 1/4*	*h = 1/6*	*h = 1/8*	*h = 1/10*
Exact for P-2 (3 nodes)	2.939394693E-5	1.465421827E-5	1.112837818E-5	9.622897451E-6	8.854582211E-6
Exact for P-3 (7 nodes)	3.066515034E-6	1.402741081E-6	8.127623607E-7	5.751547558E-7	5.243351400E-7
Exact for P-4 (6 nodes)	1.053361544E-6	7.307525941E-7	1.255049310E-6	1.665202089E-6	1.977574500E-6
Exact for P-6 (12 nodes)	1.022903144E-9	1.125287218E-8	4.931667438E-8	1.426724375E-7	3.123004157E-7
Exact for P-8 (16 nodes)	9.70062571E-10	1.078406109E-8	4.742161118E-8	1.376452068E-7	3.131926566E-7
Exact for P-9 (22 nodes)	9.693837900E-10	1.078261173E-8	4.741882419E-8	1.376404249E-7	3.131852676E-7

Figure 4b. — P_2-Lagrange edge/Sander.

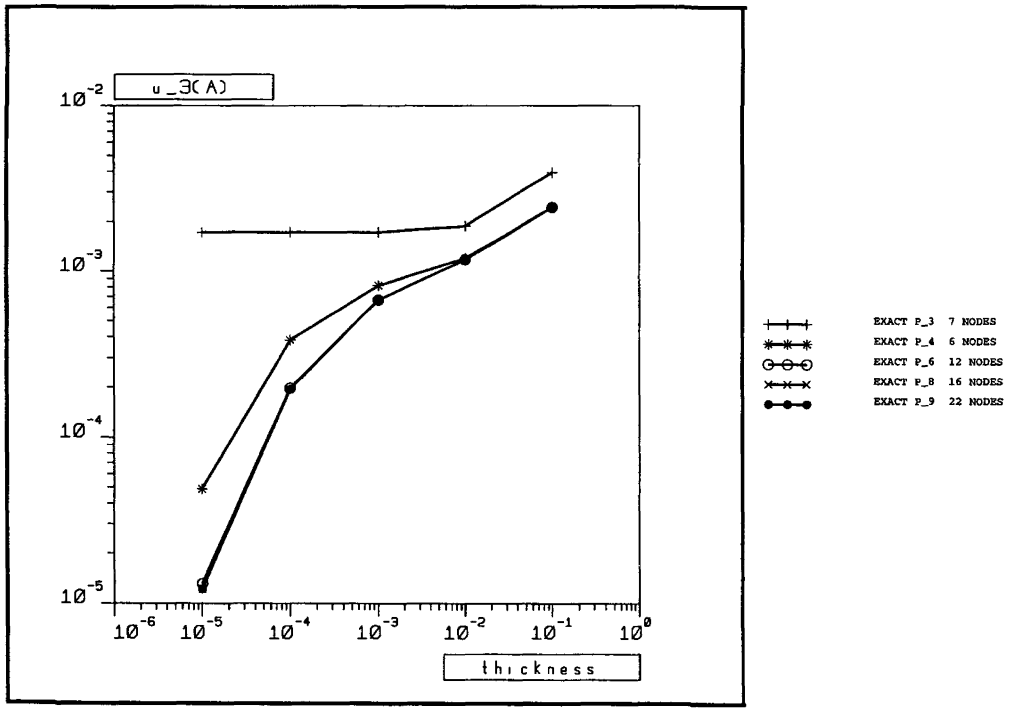

Figure 5c. — Ganev-Argyris, h = 1/2.

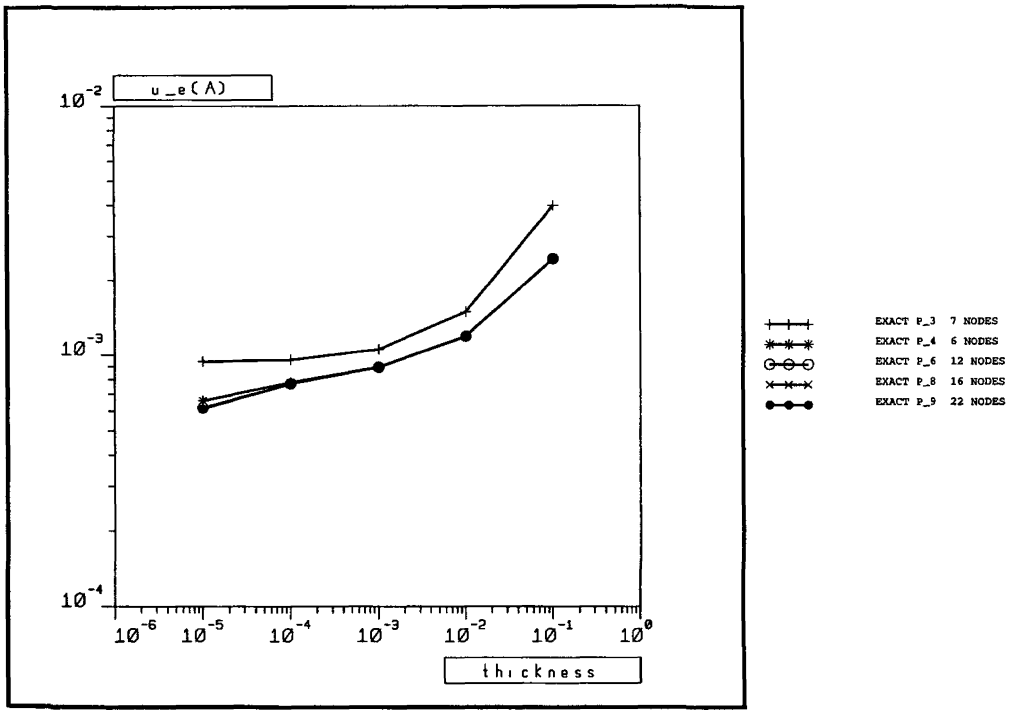

Figure 5d. — Ganev-Argyris, h = 1/10.

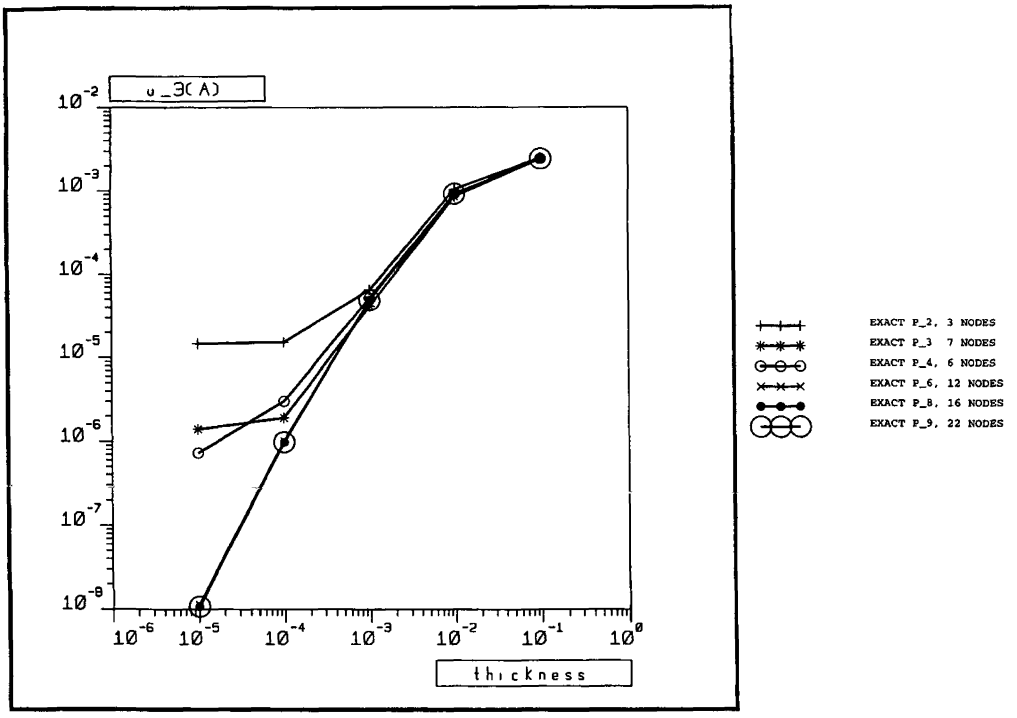

Figure 5e. — Sander, h = 1/4.

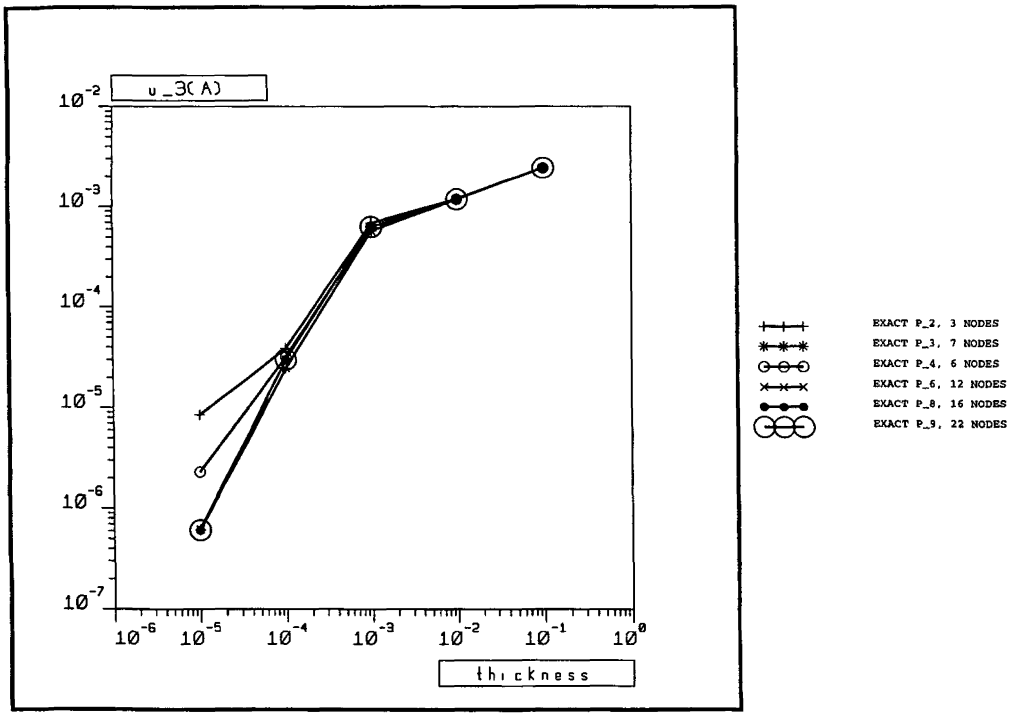

Figure 5f. — Sander, h = 1/12.

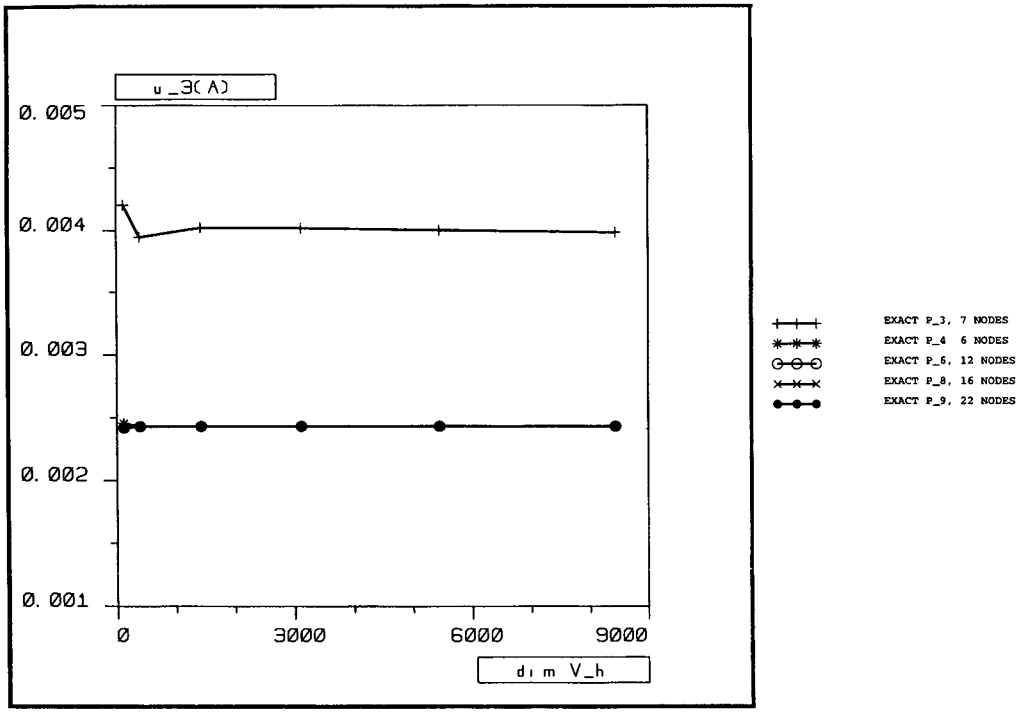

Figure 6g. — Ganev-Argyris, $\varepsilon = 10^{-1}$.

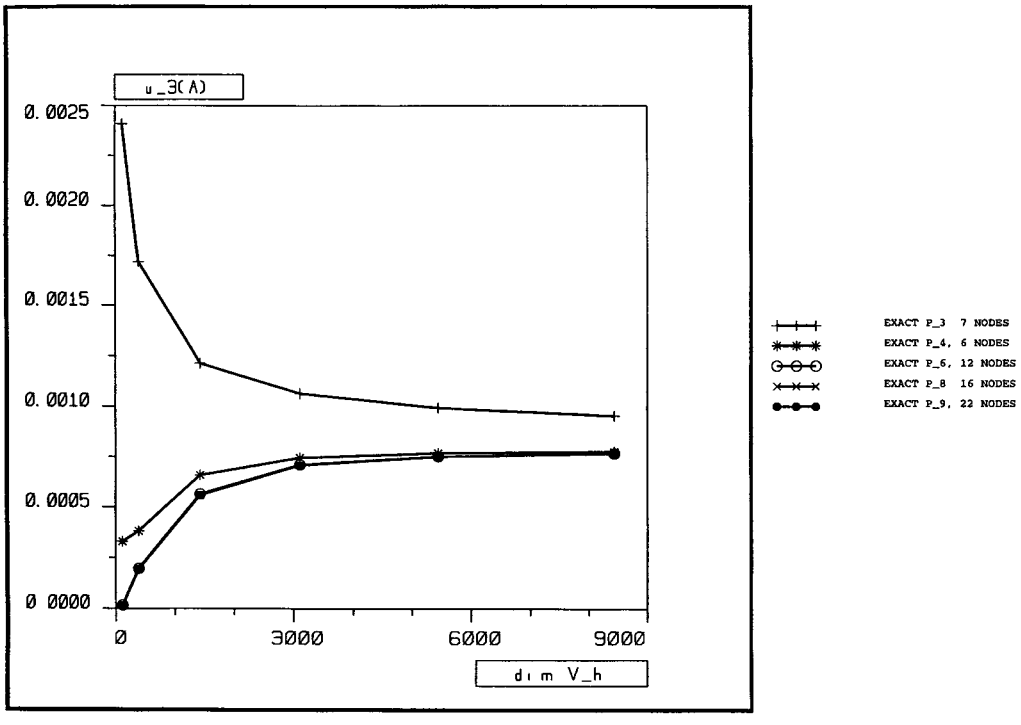

Figure 6h. — Ganev-Argyris, $\varepsilon = 10^{-4}$.

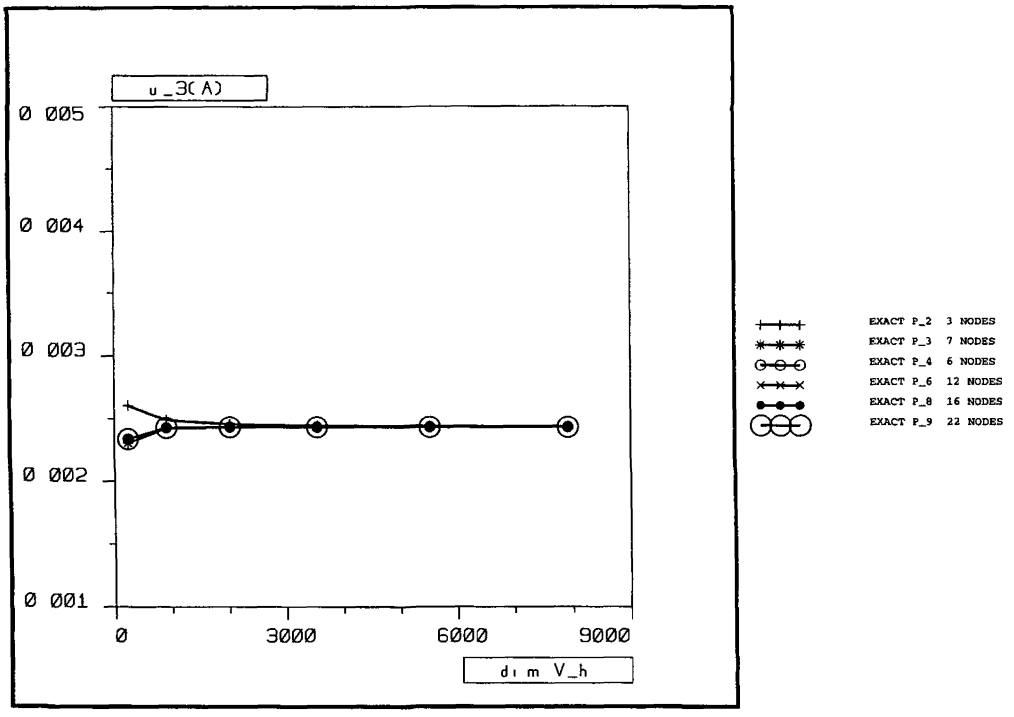

Figure 6i. — Sander, $\varepsilon = 10^{-1}$.

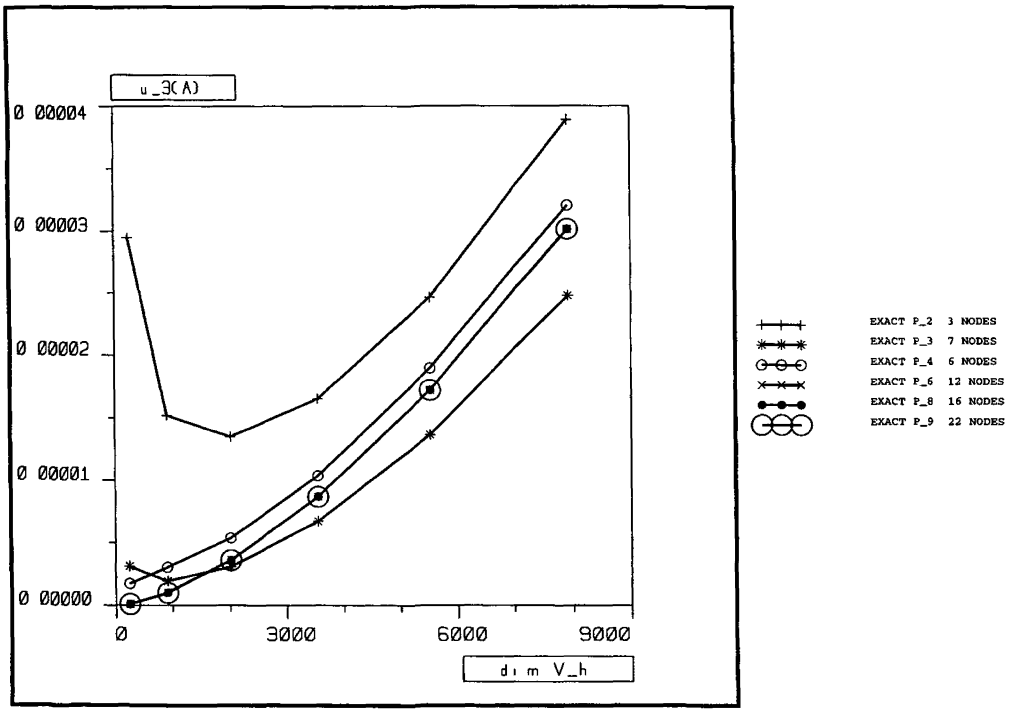

Figure 6j. — Sander, $\varepsilon = 10^{-4}$.

We also point out that the differences due to the reduced integration schemes are insignificant and only for ε "very small" we find some differences; consequently we conclude that the membrane locking is not eliminated when we use a reduced integration scheme (we observe that some low precision schemes eliminate the locking but the corresponding results are wrong since the convergence is not reached, see the scheme exact for P_3 in Ganev-Argyris).

REFERENCES

[1] J.L. AKIAN et E. SANCHEZ-PALENCIA, "Approximation des coques élastiques minces par facettes palnes. Phénomène de blocage membranaire", *Compt. Rend. Acad. Sci. Paris,* **315,** p. 363-369 (1992).

[2] I. BABUSKA and M. SURI, "On locking and robustness in the finite element method", *SIAM Jour. Numer. Anal.,* **29,** p. 1261-1293 (1992).

[3] T. BELYTSCHKO, H. STOLARSKI, W.K. LIU, N. CARPENTER and J.S.J. ONG, "Stress projection for membrane and shear locking in shell finite elements", *Comp. Meth. Appl. Mech. Engng.,* **51,** p. 221-258 (1985).

[4] M. BERNADOU, "*Méthodes d'éléments finis pour les problèmes de coques minces*", Masson, Paris (1994).

[5] M. BERNADOU and P.G. CIARLET, "Sur l'ellipticité du modèle linéaire de coques de W.T. Koiter" in *Computing methods in Sciences and Engineering,* R. Glowinski, J.L. Lions ed., p. 89-136, Lecture Notes in Econom. and Math. Systems, vol. 134 (1976).

[6] D. CHENAIS, J. C. PAUMIER, "On the locking phenomenon for a class of elliptic problems", *Num. Math.,* **67,** p. 427-440 (1994).

[7] P.G. CIARLET, "*The finite element method for elliptic problems*", North-Holland, Amsterdam (1978).

[8] G. GEYMONAT and E. SANCHEZ-PALENCIA, "On the rigidity of certain surfaces with edges and application to shell theory", *Arch. Rat. Mech. Anal.,* **129,** p. 11-45 (1995).

[9] A. HABBAL and D. CHENAIS, "Deterioration of a finite element method for arch structures when thickness goes to zero", *Num. Math.,* **62,** p. 321-341 (1992).

[10] A. KALMOULAKOS, "A Catenoidal patch test for the inextensional bending of thin shell finite elements", *Comput. Meth. Appl. Mech. Engng.,* **92,** p. 1-32 (1991).

[11] F. KIKUCHI, "Accuracy for some finite element models for arch problems", *Comput. Meth. Appl. Mech. Engng.,* **35,** p. 315-345 (1982).

[12] J.N. Lyess and D. Jespersen, "Moderate degree symmetric quadrature rules for the triangle", *Jour. Inst. Math. Appl.,* **15,** p. 19-32 (1975).

[13] F. NIORDSON, "*Shell Theory*", North-Holland, Amsterdam (1985).

[14] J. PITKARANTA, "The problem of membrane locking in finite element analysis of cylindrical shells", *Num. Math.,* **61,** p. 523-542 (1992).

[15] E. SANCHEZ-PALENCIA, "Statique et dynamique des coques minces. I: Cas de flexion pure non inhibée", *Compt. Rend. Acad. Sci. Paris,* série I, **309,** p. 411-417 (1989).

[16] E. SANCHEZ-PALENCIA, "Statique et dynamique des coques minces. II: Cas de flexion pure inhibée, approximation membranaire", *Compt. Rend. Acad. Sci. Paris,* série I, **309,** p. 531-537 (1989).

[17] E. SANCHEZ-PALENCIA, "Asymptotic and spectral properties of a class of singular-stiff problems", *J. Math. Pures Appl.,* **71,** p. 379-406 (1992).

[18] E. SANCHEZ-PALENCIA, "On the membrane approximation for thin elastic shells in the hyperbolic case", *Rev. Mat. Uni. Comp. Mad,* **6,** p. 311-321 (1993).

[19] E. SANCHEZ-PALENCIA, "Surfaces et coques élastiques minces: problèmes et défis", *La Vie des Sciences,* **12,** p. 239-258 (1995).

[20] L. SCHWARTZ, "*Cours d'Analyse, vol. I*", Hermann, Paris (1981).